Heliyon 10 (2024) e39948

Contents lists available at ScienceDirect

Heliyon

journal homepage: www.cell.com/heliyon

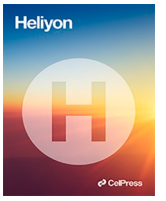

Research article

Spatiotemporal distribution, environmental correlation and health risk analysis of *Culex tritaeniorhynchus* (Diptera: Culicidae) in Beijing, China

Mei-DE. Liu [a], Qiu-Hong Li [a], Ting Liu [a], Xiu-Yan Xu [a], Junqi Ge [b], Tong-Yan Shen [c], Yun-BO. Wang [d], Xian-Feng Zhao [e], Xiao-Peng Zeng [a], Yong Zhang [a,*], Ying Tong [a,**]

[a] *Beijing Municipal Center for Disease Prevention and Control, Beijing, 100013, China*
[b] *Chaoyang District Center for Disease Control and Prevention, Beijing, 100021, China*
[c] *Xicheng District Center for Disease Control and Prevention, Beijing, 100020, China*
[d] *Dongcheng District Center for Disease Control and Prevention, Beijing, 100009, China*
[e] *Tongzhou District Center for Disease Control and Prevention, Beijing, 101100, China*

ARTICLE INFO

Keywords:
Culex tritaeniorhynchus
Spatiotemporal
Distribution
Environment
Urban

ABSTRACT

The *Culex tritaeniorhynchus* Giles, 1901 (Diptera: Culicidae) is major vector of Japanese encephalitis (JE) in China, and this study aimed to uncover the vector's spatiotemporal distribution and environmental correlation in Beijing. In study area, the Remote Sensing (RS), Global Position System (GPS), and Geographic Information System (GPS) were used to clarify the distribution characteristics of vector on spatial and temporal scales, and regressions analysis of cross-sectional study was performed to detect the environmental factors linked with the density and presence of *Cx. tritaeniorhynchus*. In study area, the scenic area was the major environmental area for breeding of the vector, August was the primary peak month, the new urban development area (NUDA) was major distribution subarea of Beijing, and the vector could be detected throughout the subarea of Beijing from June to September. In the scenic area, the total value of light index within buffer zones of 100 m (LT_100) and the total value of NDVI index within buffer zones of 800 m (NDVI_800) determined whether there was a positive or negative vector in the trapping sites, and the total value of NDVI index within buffer zones of 100 m (NDVI_100) and LT_100 was linked to the density of the vector. Our findings provide better insight into the spatio-temporal distribution pattern, associated environmental risk factors, and health risk of vector in Beijing. Based on the results here, we could predict the risk of JE and create and implement location-specific JE prevention and control measures to prevent future risks during the urbanization advancement of Beijing.

1. Introduction

As one of the essential endemic encephalitis, Japanese encephalitis (JE) affects over 50,000 patients and results in 15,000 deaths annually in Eastern and Southeastern Asia [1,2]. Despite increasing vaccination to fight JE, JE cases in China still account for 50 % of

* Corresponding author.
** Corresponding author.
E-mail addresses: zhangycdc@126.com (Y. Zhang), tongying96@126.com (Y. Tong).

https://doi.org/10.1016/j.heliyon.2024.e39948
Received 23 July 2024; Received in revised form 27 October 2024; Accepted 28 October 2024
Available online 29 October 2024

the reported JE cases worldwide [3]. The *Culex tritaeniorhynchus* (Giles, 1901) transmit the virus by biting, and JE occurs most commonly in agricultural areas being provided with pig and rice paddies [4]. Moreover, JE may also circulate in a broader range of environments, given the diversity of its potential hosts [5].

The arthropod-borne viruses, including JE, have spread more widely and infected larger populations in recent decades, [6]. The expansion of arthropod-borne diseases is closely associated with urbanization, climate change, and human activities that create a more permissive environment for transmission [7,8]. In Janpanes downtown area, 5 % of the urban population acquired natural JE virus infection in 1981 and 1995 [9]. Similarly, JE cases were reported and its transmission potential cannot be igored in Vietnam [10,11], Cambodia [5] and China [12]. These previous studies not only confirm JE transmission across predominantly urban areas, and also support a greater emphasis on JE cases' finding, diagnosis, and prevention in the downtown area [13].

Generally, the urban environment is supposed to be more fittful for dengue, West Nile virus, Chikungunya viruses, and malaria due to involvement of native vector species during the transmission of these diseases in urban areas [14]. Moreover, the vector in an urban area also presents the ecological characteristics of the city (pig [15], dog [16], livestock [17], human habitations [18], and water bird [19]) that can impact the population of the vector. Thus, the mosquito vector was highlighted as public health challenges for city residents during urbanization. However, JE is considered a rural disease because of its relationship with paddy fields (vector larva breeding sites) and pigs (animal hosts of the JE virus) in countryside. Therefore, the vector of JE must be linked to very environmental factors different from that in the context of countryside.

From view point of environmental epidemiology, the distribution of JE cases and vector was significantly affected by temperature, relative humidity, wind velocity, El Nino-Southern Oscillation, and coniferous forest coverage [20]. Also, the epidemiology of urban JE is associated with social factors, such as the gross domestic product per capita, urbanization level, and land development [21,22]. Consequently, the soci-environmental factors are closely associated with distribution of the risk of JE transmission and vector simultaneously in urban area [23]. Consequently, the space-time distribution of JE cases and its vector would also display a particular pattern in urban area, which is different from that in countryside [22]. Thus, understanding the disease's spatial and temporal distribution is essential for planning and implementing of location-specific JE prevention and vector's control measures in urban areas [24].

As one kind of mosquito-borne disease, the vector was a key factor impacting JE's circulation. The number of JE patients was associated with the occurrence and density of vector [25], and the density of the vector was a good indicator of the risk of human infection [26]. For the JE, supplying JE surveillance datasets, mapping the JE risk factors contextualizes, and forecasting risk factor changes for JE may be essential for developing effective transnational health policies [27]. For the vector, the distribution map of vector could be forecast with its correlating environmental factors [28]. Therefore, measuring the vector distribution pattern and incorporating correlation environmental factors is crucial for measuring and predicting the risk of JE in urban areas.

. Beijing is China's capital city, and the JE case and its vector were reported in the downtown area [12,29]. While the spatio-temporal distribution characteristics of the vector on the city scale were unclear, and the association between the vector and the environmental factor is still absent. Based on previous research, it is safe to infer that the vector could breed in the central area of Beijing and JE transmission may also occur in urban areas, although JE cases in the central area of Beijing are rare. Nevertheless, the risk of JE is also unclear during the fast urbanization of Beijing. Thus, this study will reveal the spatial and temporal distribution characteristics of the vector and the association of the vector density with environmental factors, which could assist on JE risk prevention and vector control in Beijing.

In this study, we surveyed the density of the vector with light trapping, quantified the environmental factors with 3S technology together with satellite and remote sensing datasets, and applied logistical and linear regression to correlation analysis between the environmental factors and the vector density as well as the presence of vectors. Our findings provide better insight into the spatial distribution, associated environmental factors and health risk of vector. At the same time, there is no existing research to map an early warning of the risk of JE in Beijing city, and assessing the risk of JE based on environmental features is still difficult in rare JE cases in urban areas. Thus, the distribution and density of the vector based on satellite and remote sensing datasets would also assist in JE risk evaluation.

2. Materials and methods

2.1. Study design and vector trapping

As the Chinese capital city, Beijing is divided into four subareas with different functions, according to Beijing's main functional area planning in 2012. First, the Capital Functional Core Area (CFCA), located in the center area of Beijing, is the core capital function bar area that acts as the national center of politics, culture, and the international community, together with its long history. Second, the Urban Functional Development Area (UFDA), being contiguous to the CFCA, is the crucial area that implements and expands the capital function of Beijing. Third, the New Urban Development Area (NUDA), next to the UFDA and significantly located in south-eastern Beijing, is not only the primary carrier of manufacturing and modern agriculture but also the critical area for the decentralization of industry and population from the CFCA. Fourth, the Ecological Conservation and Development Area (ECDE), next to the UFDA but significantly located in the northwest of Beijing, is the environmental shelter and public leisure area for the capital and plays a crucial role in the sustainable development of Beijing. According to the spatial distribution characteristics of JE cases and their vectors in four subareas of Beijing, this study selected the CFCA (including Dongcheng and Xicheng districts), UFDA (Chaoyang district), and NUDA (Tongzhou district) as the study areas (Fig. 1).

In study sites, the vector is usually found in human resident (HR) areas and scenic area (SC) according to regular mosquito

surveillance (Fig. 1). From CFCA to NUDA, the sample areas of HR and SC were selected randomly, and light trapping sites were located randomly in each sample area. Finally, this study used ninety-one light traps, with fifty-two lights in the HR area and thirty-nine in the SC area. On the level of functioning district, thirty-nine lights belong to the CFCA area, thirty-two lights belong to UFDA, and twenty lights belong to NUDA.

In Beijing, the *Cx. tritaeniorhynchus* could be seen in June, July, August, and September. Therefore, vector was trapped continuously over a 7-d period in the middle of each month from 2013 to 2014. We trapped vector with light traps with carbon dioxide (MD-1 CO2 mosquito light trap 6 V/4.5AH, Beijing Logon Sci. & Tech. Co., Ltd, Beijing, China). At each light site, one light trap was hung 1.5 m above the floor, and the light was turned on at 7:00 p.m. and off at 7:00 a.m. daily. In the case of bad weather days, trapping was extended to one more day. Every day, the mosquito samples were collected and transported to the laboratory for later identification, and the trapped female mosquitoes were identified by morphology [30] and counted.

The vector density (N) was calculated from the light trap density as follows:

$$N = \frac{MN}{LN}$$

where MN is the number of trapped vectors, LN is the number of light traps, and the unit of vector density is the number of vectors per trap (NMPT).

2.2. Light-index dataset

The light-index dataset was downloaded from the NOAA website (http://ngdc.noaa.gov/eog/viirs/download_viirs_ntl.html), and light-index datasets of Beijing city were produced by intersecting the Beijing administration vector file with the downloading light-index map from NOAA.

2.3. GPS, RS, and GIS analysis of the study site image dataset

An administrative map of Beijing was obtained from the National Geomatics Center of China (https://www.webmap.cn/main.do?method=index). The administrative map contained geographic factors such as districts' administrative areas, roads, rivers, and county and provincial boundaries. Using GPS datasets of the Beijing administrative map, we ordered the TM (Landsat ETM) coverage of Beijing from EarthView Image Inc. (Beijing, China). Based on the TM datasets, the NDVI (Normalized Difference Vegetation Index), FC (vegetation Fractional Cover) and MNDWI (Modified Normalized Difference Water Index) were also generated by way of band math with the Orfeo Toolbox in QGIS 3.22.5. These remote sensing environmental indices were selected because they index the water body and vegetation situation and link to JE's breed of the vector.

2.4. Extraction of spatial factors

Using vector buffer tools in QGIS, circular buffer zones of different sizes were drawn around each light trap site based on the TM

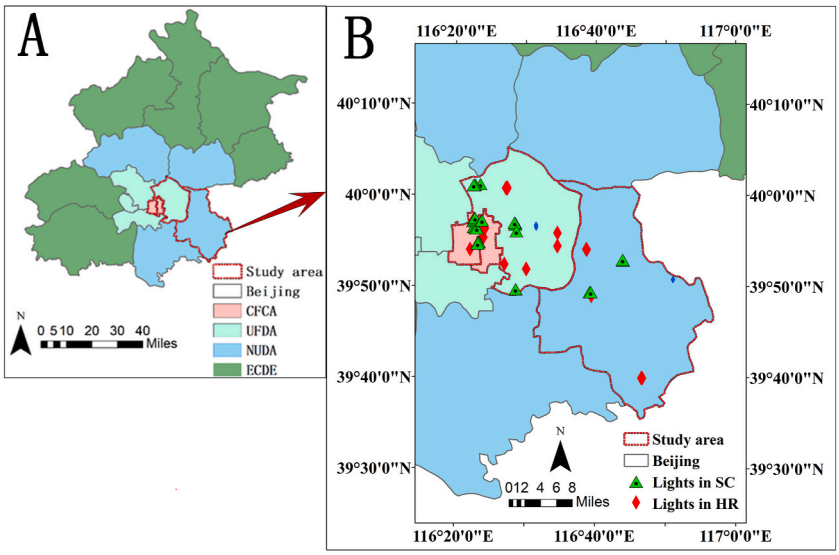

Fig. 1. Map of the study area and trapping sites. (A) Study area in Beijing including the sub-area of Capital Functional Core Area (CFCA), Urban Functional Development Area (UFDA), New Urban Development Area (NUDA), and Ecological Conservation and Development Area (ECDE). (B) Trapping sites in scenic areas (SC) and human resident (HR) areas.

image data, known local site factors, and mosquito dispersal ability. To analyze the effect of remote sensing environmental features (including NDVI, FC, MNDWI) and light (LT) index values on vector density in trap sites, hypothetical buffer distances of 100 m, 200 m, 400 m, 600 m, 800 m, 1 km, 2 km, 3 km, 4 km, and 5 km were compared. The remote sensing environmental feature datasets inside each trap site's buffer area were generated through spatial extraction with the "Zonal statistics" tool in QGIS. The remote sensing environmental features analyzed for correlation with vector abundance are listed in Table 1.

2.5. Statistical analysis

The vector density datasets were grouped on the scales of environmental type, subarea, trapping month, and trapping month within subarea, respectively. Then, the descriptive statistics and ANOVA were used to elucidate the variance in vector density in each group on different spatial and temporal scales, and Student–Newman–Keuls analysis was used to perform the two-by-two comparison among variances in each group.

On each trap site, whether a vector occurrence follows the binomial distribution and the density of the vector follows the normal distribution. Therefore, logistic regression was used to detect the occurrence risk of vector breeding related to the environmental background, and a linear regression model was adopted to find the environmental features correlating to the vector density in the light trap. Firstly, the environmental factors were first subjected to correlation analysis with the vector density; secondly, the factors displaying a significant correlation were involved in the regression model. In the logistic regression analysis, the environmental variables were introduced into the model in a "Forward-LR" way, and the environmental variables were introduced into the multiple regression model in a "stepwise" manner where the model took the density as a dependent variable model. In this study, the sample size of the regression on the vector in SC area was 39. In order to ensure appropriate statistical power of regression analysis, the number of environmental variables that were introduced into the regression model must be no more than 4 according to the Events per variable (EPV) rule [31,32].

The statistical analysis was conducted with IBM SPSS Statistics for Windows, version 19.0 (IBM Corp., Armonk, N.Y., USA), and the statistical significance was set at $P < 0.05$.

3. Results

3.1. Mosquito trapped in study

Totally, we trapped 15,490 mosquitoes with light traps, including *Cx. tritaeniorhynchus*, *Cx. pipens pallens* (Coquillett, 1898), and *Ae. Albopictus* (Skuse, 1894). The number and percentage of these species were ranked as *Cx. pipens pallens* (14,711, 94.74 %), *Cx. tritaeniorhynchus* (483, 3.12 %), and *Ae. Albopictus* (296, 1.91 %).

3.2. Vector density in the environmental type area of study area

First, we compared the vector's mean density in environment type and listed the result in Fig. 2. The mean density of the vector in the scenic area (SC) (10.33 NMPT) was significantly higher than that in the human residential area (HR) (1.54 NMPT), that is the density in the scenic area was almost five times that in the residential area. Nevertheless, the F test (ANOVA) indicated that there were statistically significant differences between the vector density in scenic and human residential areas ($F = 5.747$, $p = 0.019$). Thus, the scenic area was the primary area for infestation by vectors.

3.3. Vector density in the SC of subarea in study area

Then, we compared the mean density of vectors in SC of three subareas of the study area, and the results are listed in Fig. 3. Throughout the study period, the mean vector density in the NUDA (40.75 NMPT) was more extensive than those in the UFDA (6.25 NMPT) and CFCA (0.11 NMPT). The vector density in NUDA was almost seven times larger than that in UFDA, and the vector number in CFCA was close to zero. After ANOVA among the three subareas groups, the difference in vector density of the three regions was statistically significant ($F = 11.415$, $p < 0.001$). Furthermore, SNK analysis results displayed significant difference between two

Table 1
Definitions of environmental factors tested for correlation with vector density.

Variable	Definition
NDVI_100/200/400/600/800/1K/2K/3K/4K/5K	The total value of NDVI index within buffer zones of 100 m, 200 m, 400 m, 600 m, 800 m, 1 km, 2 km, 3 km, 4 km, and 5 km around trap sites, respectively
FC_100/200/400/600/800/1K/2K/3K/4K/5K	The total value of FC index within buffer zones of 100 m, 200 m, 400 m, 600 m, 800 m, 1 km, 2 km, 3 km, 4 km, and 5 km around trap sites, respectively
MNDWI_100/200/400/600/800/1K/2K/3K/4K/5K	The total value of NDWI index within buffer zones of 100 m, 200 m, 400 m, 600 m, 800 m, 1 km, 2 km, 3 km, 4 km, and 5 km around trap sites, respectively
LT_100/200/400/600/800/1K/2K/3K/4K/5K	The total value of light index within buffer zones of 100 m, 200 m, 400 m, 600 m, 800 m, 1 km, 2 km, 3 km, 4 km, and 5 km around trap sites, respectively

NDVI, Normalized Difference Vegetation Index; *FC*, vegetation Fractional Cover; *MNDWI*, Modified Normalized Difference Water Index; *LT*, light.

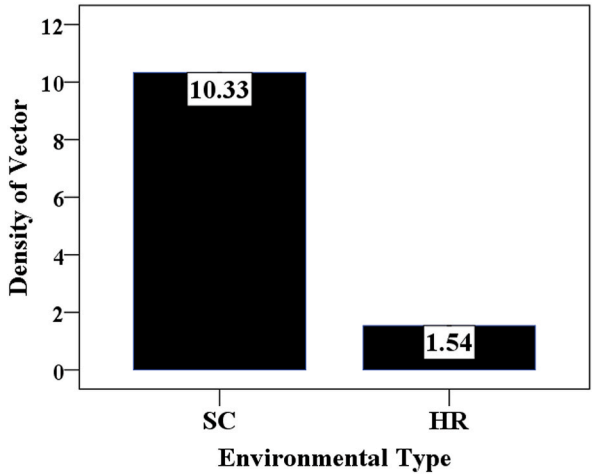

Fig. 2. Vector density comparison in the scenic areas (SC) and human resident (HR) areas of Beijing.

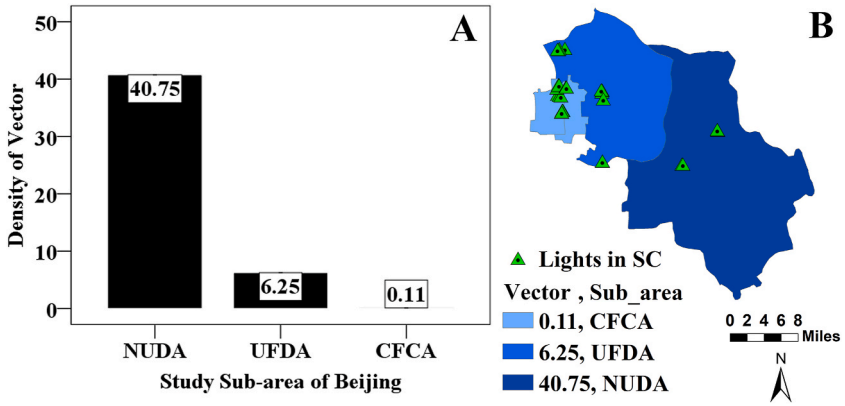

Fig. 3. Vector density comparison of scenic area (SC) among Beijing's sub-area of Capital Functional Core Area (CFCA), Urban Functional Development Area (UFDA), and New Urban Development Area (NUDA). (A) Value comparison. (B) Map of the value comparison.

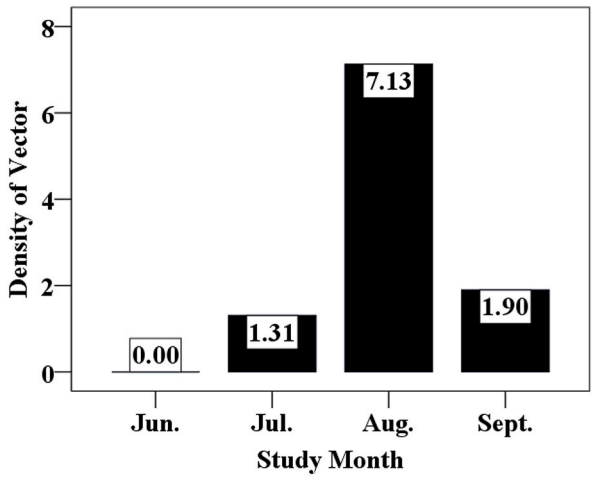

Fig. 4. Vector density comparison of scenic area among trapped months.

groups; the first group included the CFCA and UFDA, and the second group had only NUDA. According to SNK analysis, the vector number of vectors in the NUDA area was statistically significantly higher than that in the CFCA and UFDA areas, and there was no statistically significant difference between the CFCA and UFDA areas. Although the density was low in UFDA and CFCA, Fig. 3 still mention us that the vector could breed in well development urban area of Beijing, including the capital center area.

3.4. Vector density of SC in trapped months

As shown in Fig. 4, the vector densities in June, July, August, and September were 0.00 NMPT, 1.31 NMPT, 7.13 NMPT, and 1.90 NMPT, respectively. No vector could be detected in June. The vector density in August was five times and four times larger than those in July and September, respectively. Thus, August was the top season, and July and September were the second distribution months. Moreover, ANOVA showed that the mean difference over four months was statistically significant ($F = 4.369$, $p = 0.005$); Student–Newman–Keuls analysis showed that the vector density in four months could be subdivided into two groups in which there was no statistically significant difference among each month. The first group included June, July, and September, and the second group included only August. Thus, the density in August was significantly more extensive than those in June, July, and September.

3.5. Vector density of SC in subarea during trapped months

First, we grouped the vector density into four months in CFCA, UFDA, and NUDA, resulting in twelve group means of vector density. As shown in Fig. 5-I, the vector density in August of NUDA (32.63 NMPT) was listed as the highest among all means. The vector density in July of NUDA (6.38 NMPT) was second. The vector densities in September of UFDA, September of NUDA, August of UFDA, and September of CFCA were 4.83 NMPT, 1.75 NMPT, 1.42 NMPT and 0.11 NMPT, respectively. The ANOVA analysis showed significant differences among the 12 groups' vector densities ($F = 9.78$, $p < 0.001$); the Student–Newman–Keuls analysis results displayed significance among the two groups. The first group included June-NUDA, July NUDA, Sep-NUDA, June-UFDA, July UFDA, Aug-UFDA, Sep-UFDA, June-CFCA, July CFCA, Aug-CFCA and Sep-CFCA, and the second group included only Oct-NUDA. Thus, the vector density among June-NUDA, July NUDA, Sep-NUDA, June-UFDA, July UFDA, Aug-UFDA, Sep-UFDA, June-CFCA, July CFCA, Aug-CFCA, and Sep-CFCA was nonsignificant, and those densities were significantly lower than that in Aug-NUDA.

Also, we map the vector density of SC of three subareas of study area in four months in Fig. 5-II. As Fig. 5-IIshown, there was no vector trapped in all three subareas in June (Fig. 5-II-A), there was vector only in NUDA (6.38 NMPT) in July (Fig. 5-II-B), there was no vector in CFCA and higher vector of NUDA(32.60 NMPT) than that in UFDA (1.42 UFDA) in August (Fig. 5-II-C), and there was higher vector of UFDA (4.83 NMPT) than that of NUDA (1.75 NMPT) and CFCA (0.11 NMPT) (Fig. 5-II-D).

3.6. Mapping spatiotemporal distribution of vectors in scenic area

The trapping sites in scenic area are shown in Fig. 6(A), and the positive vector sites in June, July, August, and September are displayed in Fig. 6(B) and. 6 (C), Fig. 6(D) and 6 (E). In June, we could trap the vector in all scenic area sites, which corresponds well

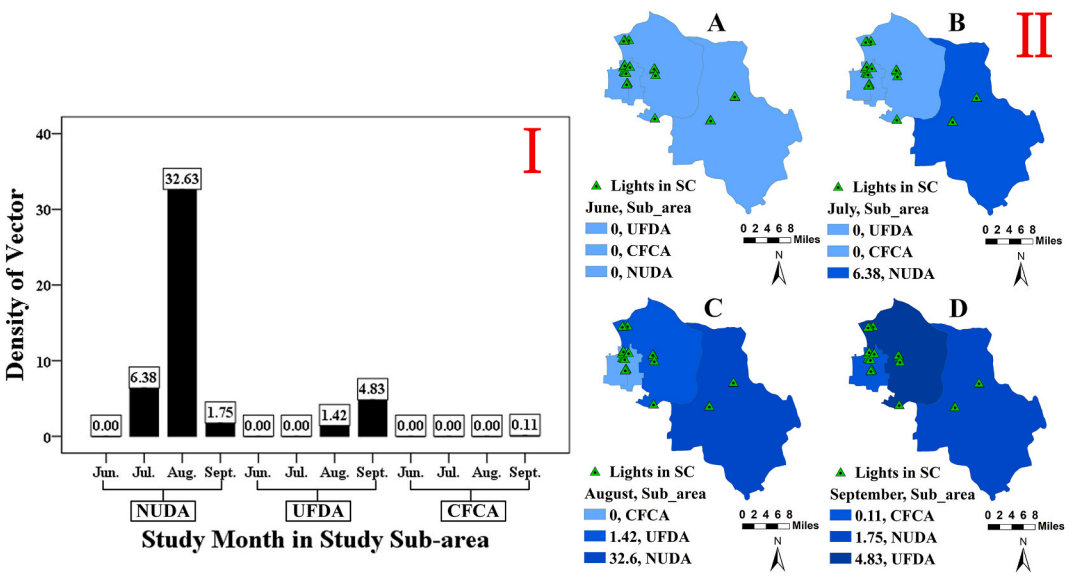

Fig. 5. Vector density comparison of scenic area among Capital Functional Core Area (CFCA), Urban Functional Development Area (UFDA), and New Urban Development Area (NUDA) in trapped months. (I) Value comparison. (II) Map of the value comparison in June(A), July(B), August(C) and September(D).

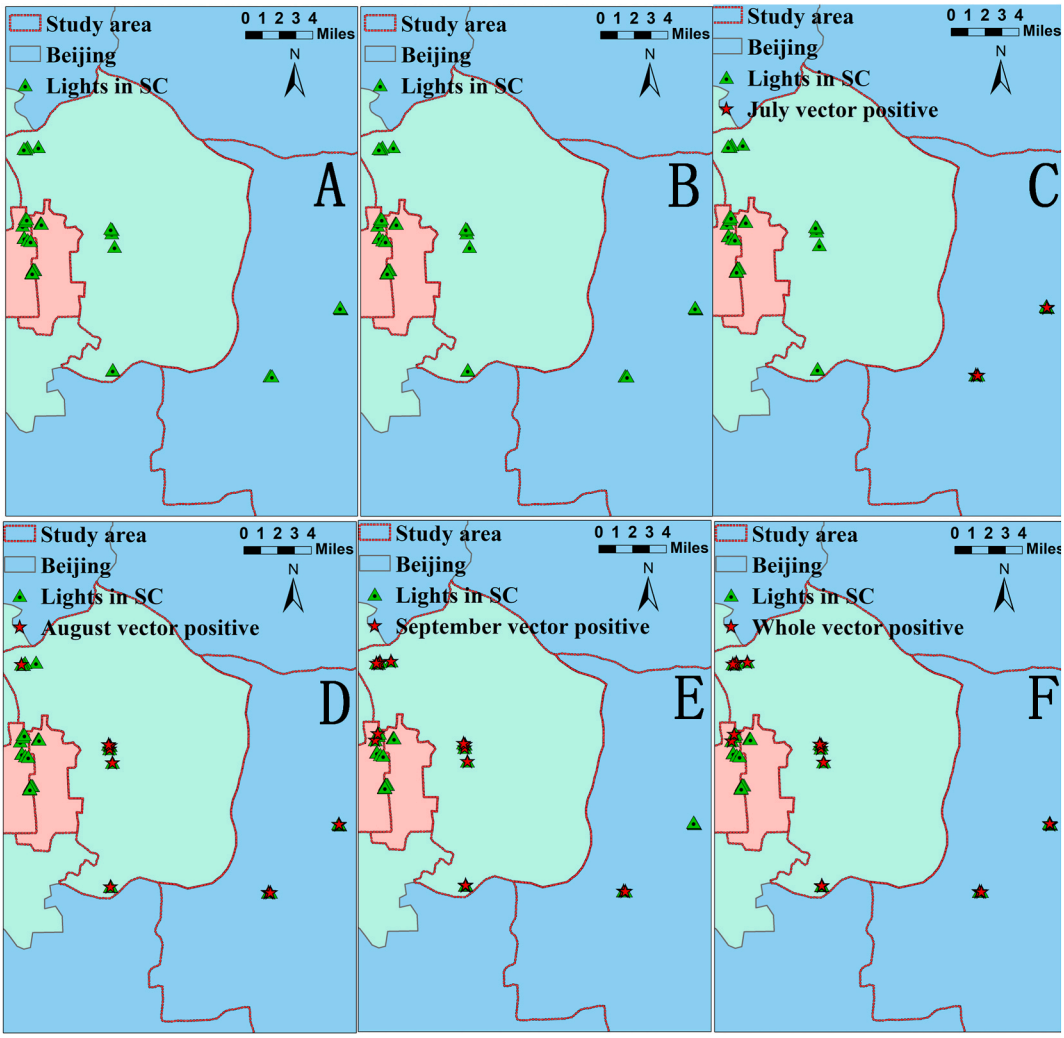

Fig. 6. Spatial-temporal distribution dynamic map of vectors' positive sites in scenic area. (A) Vectors' positive sites in scenic area. (B) Vectors' positive sites in June. (C) Vectors' positive sites in July. (D) Vectors' positive sites in August. (E) Vectors' positive sites in September. (F) Whole vectors' positive sites in study area.

with the density results above. However, the vector could be detected in July NUDA, August NUDA and UFDA, and all three regions in September with many blank vector sites. Fig. 6 (F) shows the positive scenic area of the entire study period. The vector could be detected as positive in many locations, except for some zero areas in the CFCA. In summary, there was a clear distribution pattern transition of the positive vector site from Fig. 6 (A) to Fig. 6 (E). From July to September, the positive vector sites expanded from NUDA to UFDA and CFCA.

3.7. Logistic regression analysis of the positive or negative vectors in scenic area

Fig. 6 (F) shows that some scenic area in the CFCA trapped zero vectors throughout the study period. Thus, there was a one versus

Table 2
Logistic regression analysis on the positive or negative of vectors in scenic area.

Model	B	df	Sig.	Exp (B)	EXP(B) 的 95 % C.I.	
					Lower limit	Upper limit
LT_100	−2.343	1	0.011	0.096	0.016	0.587
NDVI_800	1.688	1	0.013	5.407	1.424	20.535
Constant	−0.004	1	0.992	0.996		

LT_100, total value of light index within buffer zones of 100 m; *NDVI_800*, total value of NDVI index within buffer zones of 800 m.

zero (one stands for vector positive and 0 for zero vector in sites) chance of the vector detected in the scenic area. It is convenient to perform logistic regression to reveal whether and what environmental features could contribute to the detected vector. As shown by logistic regression (forward stepwise (LR)) (Table 2), NDVI_800 and LIHT100 could be included in the regression model (Hosmer–Lemeshow test, $X^2 = 5.4529$, $p = 0.806$). The LT_100 was negatively related to whether the vector was caught in the scenic area (OR: 0.096, 95%CI: 0.016–0.587, $p = 0.011$), and the NDVI_800 was positively correlated with the vector being detected in scenic area (OR: 5.407, 95%CI:1.424–20.535, $p = 0.013$). The number of environmental variables that were introduced into the regression model was smaller than 4, which would ensure appropriate statistical power of regression analysis according to the EPV rule.

3.8. Linear regression analysis of the vector density with environmental factors

Additionally, linear regression (in a forward stepwise way) was performed to analyze the relationship between vector density and environmental features. As a result (Table 3), NDVI_100 and LT_100 could be included in the final linear model ($F = 8.375$, $p = 0.001$). Moreover, NDVI_100 ($B = 0.200$, $t = 2.797$, $p = 0.008$) was positively correlated and LT_100 ($B = -0.257$, $t = -3.579$, $p = 0.001$) was negatively correlated with vector density. Finally, the vector density in each scenic area could be simulated by a linear model as follows:

$$D = 0.485 + 0.200*NDVI\_100 - 0.257*LT\_100$$

where D is the vector density in trapping sites. The number of environmental variables that were introduced into the regression model was smaller than 4, which would ensure appropriate statistical power of regression analysis according to the EPV rule.

4. Discussion

In present paper, the vector preferred the scenic areas (SC), and the vector could be detected in SC sites of CFCA, UFDA, and NUDA. The vector is generally considered a mosquito in the countryside and peri-urban regions [33], and the JE's infection force is identical in the peri-urban and rural farm regions. Previous studies observed breeding of vector in the urban subchannel system of Beijing [29] and the residential area of Nanjing [34]. Thus, the present paper confirmed the scenic area' critical role in sustaining the vector population, although a typical JE animal host (pig for example) was lacking in the urban area of Beijing. During the vector survey in Beijing, scenic area included parks, scenic spots, and public lawns [35]. In these scenic area, the state and clear water or the urban water in channels could sustain vector breeding very well, the thriving planting around the lake or channels provides the best-rested sites for vector adults, and city animals (birds, for example) may also take the place of pigs (in the countryside) as animals' blood animals for vectors. Thus, scenic area has the most similar environmental character for breeding as that in the suburban area. Therefore, it is safe to conclude that the scenic area of Beijing could sustain vector establishment in urban areas belonging to specific breeding sites in the countryside with the advancement of urbanization in the city. The city's scenic area determined the extent of the vector and its borne diseases in the urban area [14]. Compared with the environment in the countryside, the metropolitan region representing a more complex system has distally different characteristics and typical unfitted echo for the vector (resident and business section, for example). Therefore, we reported the vector's scenic area preference in the urban area for the first time. Beijing plans to build its urban green belt with many scenic area [39], which would benefit the environment by vector infesting. Hence, this study reminded us of the risk of vector breeding and told us that survey and control measures should be applied to demolish the risk of JE transmission in urban areas.

In this study, the vector was primarily detected in the new urban development area (NUDA) of Beijing, which is statistically higher than that in the center (CFCA) together with intercalary area (UFDA). In the center area (CFCA), the vector density displayed non-significance against that in UFDA. The vector was distributed across the city (including the center area) and was not limited to the countryside area. Generally, the *Cx. tritaeniorhynchus* is considered a rural mosquito species because the rural environment could provide breeding sites such as rice fields, cannel, streams, and ponds [36]. The three rustic environmental elements (paddy fields, pig farms, human habitations) of JE facilitate or impede the movement of vectors and then determine how the JE interacts with hosts and vectors and the infection risk to humans ultimately [18]. In Beijing, the *Cx. tritaeniorhynchus* could be found in the downtown area [29], but that researcher did not uncover the spatial distribution of the vector among urban areas. However, this study revealed *Cx. tritaeniorhynchus* spatial distribution in three city sub-areas ranging from the center to the suburbs and confirmed the vector density distribution in the density grade in Beijing. The vector species can present in urban households with and without pigs, and keeping pigs

Table 3
Linear regression model of the vector density with geoenvironmental features in scenic area.

Model	Coefficient analysis					Model ANOVA			
	Coefficients	95 % Confidence Intervals		t	Sig.	F	Sig.	df	
		Lower Limit	Upper Limit						
Constant)	0.485	0.347	0.623	7.119	0.000	8.375	0.001	Regression	2
LT_100	−0.257	−0.402	−0.112	−3.597	0.001				
NDVI_100	0.200	0.055	0.344	2.797	0.008			Residual	36

LT_100, total value of light index within buffer zones of 100 m; *NDVI_100*, total value of NDVI index within buffer zones of 100 m.

increase vector density only [15]. Together with the present study, the *Cx. tritaeniorhynchus* had developed a stand breed site in an urban environment, although Beijing forbids the pig from growing in the metropolitan area. In the suburbs, environmental features preserve similar charters as in the countryside, and the similarity between the country and urban subregion decreases gradually closer to the city center. Therefore, the gladly decreasing vector density in this study agreed well with the breeding ecology of *Cx. tritaeniorhynchus*. In the center area of Beijing, the urban area also offers breeding sites for *Cx. tritaeniorhynchus*, such as lakes, wetlands, and ponds, which resemble *Cx. tritaeniorhynchus* breeding function to their county part in the countryside [33], which makes breeding vectors in the center area possible. In this study, the resettlement of the vector in the central area also hinted at the risk of JE in the most highly urbanized region in Beijing. Therefore, survey and control of JE and its vector should not be limited to the suburban area, while taking the all-city space for attention is necessary. The vector must find similar breeding sites in the countryside to make a living in the central urban area. Therefore, we must keep an eye on it and take the right action to survey and control its breeding in urban areas in the future.

On the level of months in CFCA, UFDA, and NUDA, the vector density in August of NUDA was listed as the highest, and September was the peak period in the UFDA and CFCA. In addition, vector density in the UFDA and CFCA showed different temporal distribution patterns from that in NUDA. Regarding the temporal distribution pattern, the previous studies only took the study area as a whole and did not uncover the distribution pattern diversity among different urban areas. Hence, this study not only revealed the temporal pattern of the vector at the city level but also revealed the other temporal distribution characteristics and diversity levels of the environment, area, and city. In the different districts of Beijing, vector density peaked in August and September in the NUDA area [37] and September in UFDA [38,39], and the JE case peak ranged from October [40] to September [41]. In this study, we also found the vector density of UFDA ranked first among three subareas of study in September. Thus, our study agreed well with the JE epidemiology characters among districts, from the point of view of vector-borne disease. At the temporal scale, climate factors account for the temporal distribution pattern of the vector [42] as well as JE cases [43]. In China, the more southern and eastern, the earlier vector density peaks, and the period is closely related to temperature ascent [44]. In our study area, the peri-urban area sites in NUDA (Tong Zhou District) are located southeast of the CFCA and UFDA, which results in an earlier warm climate than that of the CFCA and UFDA. The geographic position of the three areas may cause vector density to peak one month earlier in NUDA than in CFCA and UFDA. Overall, this study sheds light on density-peaking diversity among subareas with diverse urbanization levels. The spatiotemporal distribution of mosquitoes helped improve the understanding of the relative risk of flavivirus infection and monitoring and long-term surveillance. Therefore, the vector temporal distribution pattern would assist in preventing and controlling the vector at the right time for Beijing.

The NDVI indices the growth and coverage of vegetation and is closely related to the presence and density of the vector [45]. In this study, the NDVI was positively linked to the occurrence and density of vector at distances of 800 m and 100 m, respectively, highlighting NDVI's key role in vector breeding and resting in scenic area. The linking of the NDVI with the vector has been confirmed in China [46] and Korea [42], which are major JE-transmitting countries in Asia. As a crucial environmental factor, the impact of NDVI on the vector in Beijing's urban areas is not yet clear. Previous studies have pointed out the augmented function of NDVI on vectors. Likewise, this study confirmed the boosting sense of NDVI in the context of the city, and the vegetation in urban areas boosted the vector population and the countryside. In Beijing city, there is higher NDVI value in NUDA for the lower building construction level and in August as well as September for the reason of vegetable development pattern of local region. Besides, the scenic area is the typical vegetation planted place for afforestation, city view, and environmental purification. The plant of scenic area in an urban area plays an analogical role for the vector sustaining in the countryside. Otherwise, the vector cannot fit echo in the city background, in which suitable sites for adult resting or lava breeding shade are lacking. Hence, this study detected the vegetable factors relating to vector and quantity that impact with regression analysis, and the vegetable features also provided explains for the distribution pattern of vectors on the level of spatial and temporal. Beijing is enforcing its scenic area construction to favor vectors inhabiting the urban area. Therefore, these results could advise the indication of the hot point of the vector breeding sites and assist in controlling the vector in the urban environment. These results also suggested that we should further surveil the vegetation ecological function, which would increase our understanding of the vector ecology in the metropolitan area.

In present paper, the light index value correlated negatively with the vector's occurrence and density in the Beijing scenic area. Furthermore, the vector density decreased on the scale of sub-area along with descending urban light sources reduced gradually in NUDA, UFDA, and CFCA, which also hint the negative affection of the light index on the vector density. Light is always regarded as an attractive source for mosquitoes, and light trapping is also used widely to deter the presence or density of the vector [47]. The influence of urban light on insects has been the subject of much research, but few studies have focused on the effect of urban light on the vector of JE. So, this study elucidated the impact of the urban light level on the vector, which revealed a new effect of urban light. Therefore, the results here not only denied the attractive role of urban light but also demonstrated that urban light had a repellent effect on the vector in Beijing urban area. In metropolitan areas, the city-light indexing urban developmental level plays a crucial role in the environmental impacting on the urban insect population [48]as well as vector control [49]. In the typical well-urbanized area, concrete ground, few vegetables, and covered city water bodies constitute unsuitable circumstances for the vector. Therefore, the higher urbanization level means less similarity of the environmental characteristics to the countryside being a typical live area for the *Cx. tritaeniorhynchus*. The night-light population's negative effect on the urban ecosystem has received much attention [48], so decreasing urban light would be popular in the future. According to this study, decreasing of the urban light would increase the JE risk amount in the metropolitan area of Beijing. After all, this study not only pointed out the negative effect of light on the population of *Cx. tritaeniorhynchus* but also modeled the link between vector density and urban light index, which could help locate the hot point of vector breeding to prevent and control JE transmission in Beijing.

In addition to environmental features, spatial distance is involved in the environmental influence on the occurrence and density of

an urban vector in this study. That, the NDVI affected at distance of 800 m (occurrence) and 100 m (density), and urban light affected at distance of 100 m (occurrence as well as density). NDVI values linked to vector density were reported by many studies [42,46], but none of them declared the affecting distance of NDVI or LT on the density or occurrence of the vector. Therefore, this study shed light on the spatial ecological relationship of vegetation to the vector and quantified this relationship with regression models. The spatial distance affecting the vector has been noted, for example, the distance from breeding sites linked to vector density [50] and disease spreading range [51]. Such distance influence was related to the fly competence of the mosquito in a particular ecological context. As reported, the flight distance for a mosquito blood meal is an average of approximately 100 m [52], and Culex flies at least 900 m away [53]. In this study, the affection space distance of the NDVI and light also lie at 800 m and 100 m, and these distances were close to the flight distance of mosquitoes in previous papers. Here, we deduced that the effects of vegetation and light on the vector were effective at unique spatial scales. In other words, vegetation and light affect the vector with extended spatial distance, and such a distant influence was linked to the fly competence of the vector. In this study, the 800 m (NDVI) and 100 m (NDVI and light) coincided nicely with the flying distance of the vector. The 800 m may be the least suitable area space distance for the vector, and the 100 m was the popular fly range of the vector. Consequently, vegetation in 800-m buffers means that the acre of the scenic area around the trapping sites could sustain the breeding of the vector in its environment. Furthermore, a 100 m environmental buffer area around the trapping sites determined the occurrence and density of the vector around the trapped sites. Thus, this study would help estimate the effect distance or extent of the environmental factor on the vector, plan the position and boundary of the vector survey, and make precise control in the urban city. However, the practice of results in future prediction and control of the vector still needs to overcome more detailed fieldwork.

5. Conclusions

In China, JE is a vector-borne disease that breaks out in the countryside and suburban areas, for the reason of its vector's breeding in rice field in rural area [33]. However, JE cases have also been reported in urban areas in Japan [9], Vietnam [10], and China [12], and the spatiotemporal distribution and environmental correlation of the vector in urban area are still unknown. This study confirmed the exiting of the vector in the urban area of Beijing, particularly in the center area of the city. Second, this study scientifically described the spatial and temporal distribution characteristics of the vector in the capital city area for the first time. Finally, particular environmental features were linked to the existence and density of the vector in the ecological scenic area. For the first time, this study highlights the risk of JE in the Beijing center area and clarifies the breeding site type of the vector in the downtown area of Beijing. By adding vegetation area and decreasing the light index during the urbanization advancement of Beijing, the vector density would mount in the urban area. Thus, this paper also cautions about the JE risk, surveillance on the vector in urban area without rice field, and applying control management during the urbanization process of Beijing. Based on field trapping and 3S analysis, this study not only clarified the spatiotemporal distribution characteristics but also modeled the correlation of environmental features linked to the vector of JE. To eliminate the JE risk in the central urban area of Beijing, people should keep a close eye on the urban breeding vector and its epidemiological risk and then take corresponding and precise measures to prevent and control the vector. Nevertheless, this study also had many limitations. First, the ecological mechanism of environmental factors impacting the vector was not determined in this paper and needs further analysis. On the other hand, JE risk prediction also needs further study from the viewpoint of vector-borne disease during the urbanization advancement of Beijing because this paper focuses primarily on vector respect. Finally, an additional field study was necessary to control the vector in the urban area of Beijing.

CRediT authorship contribution statement

Mei-DE. Liu: Writing – original draft, Software, Methodology, Investigation, Conceptualization. **Qiu-Hong Li:** Methodology, Formal analysis, Data curation. **Ting Liu:** Investigation, Formal analysis. **Xiu-Yan Xu:** Investigation, Formal analysis. **Junqi Ge:** Investigation. **Tong-Yan Shen:** Investigation. **Yun-BO. Wang:** Investigation. **Xian-Feng Zhao:** Investigation. **Xiao-Peng Zeng:** Validation, Supervision. **Yong Zhang:** Funding acquisition, Methodology, Project administration, Supervision. **Ying Tong:** Validation, Supervision.

Ethical approval statement

Not applicable.

Human experiments

Not applicable.

Animal experiments

Not applicable.

Clinical trial

Not applicable.

Data availability statement

Not applicable.

Funding

This work was supported by a grant from the Capital's Funds for Health Improvement and Research (CFH 2024-2G-30116) and the Beijing Municipal Natural Science Foundation (7132038).

Declaration of competing interest

The authors declare that they have no known competing financial interests or personal relationships that could have appeared to influence the work reported in this paper.

Acknowledgements

This work was supported by a grant from the Capital's Funds for Health Improvement and Research (CFH 2024-2G-30116) and the Beijing Municipal Natural Science Foundation (7132038).

References

[1] U.K. Misra, J. Kalita, Overview: Japanese encephalitis, Prog. Neurobiol. 91 (2) (2010) 108–120, https://doi.org/10.1016/j.pneurobio.2010.01.008.
[2] S. Joe, A. Salam, U. Neogi, N.B. N, P.P. Mudgal, Antiviral drug research for Japanese encephalitis: an updated review, Pharmacol. Rep. 74 (2) (2022) 273–296, https://doi.org/10.1007/s43440-022-00355-2.
[3] Y. Zheng, M. Li, H. Wang, G. Liang, Japanese encephalitis and Japanese encephalitis virus in mainland China, Rev. Med. Virol. 22 (5) (2012) 301–322, https://doi.org/10.1002/rmv.1710.
[4] L.V. Simon, D.S. Sandhu, A. Goyal, B. Kruse, Japanese Encephalitis, 2023 Aug 28, in: StatPearls [Internet], StatPearls Publishing, Treasure Island (FL), 2023, 2024 Jan–, PMID: 29262148.
[5] J. Cappelle, V. Duong, L. Pring, et al., Intensive circulation of Japanese encephalitis virus in peri-urban sentinel pigs near phnom penh, Cambodia, plos neglect, Trop. Dis. 10 (12) (2016) e0005149, https://doi.org/10.1371/journal.pntd.0005149.
[6] S.C. Weaver, C. Charlier, N. Vasilakis, M. Lecuit, Zika, chikungunya, and other emerging vector-borne viral diseases, Annu. Rev. Med. 69 (2018) 395–408, https://doi.org/10.1146/annurev-med-050715-105122.
[7] A.P. Dash, R. Bhatia, T. Sunyoto, D.T. Mourya, Emerging and re-emerging arboviral diseases in Southeast Asia, J. Vector Borne Dis. 50 (2) (2013) 77–84.
[8] J.C. Pearce, T.P. Learoyd, B.J. Langendorf, J.G. Logan, Japanese encephalitis: the vectors, ecology and potential for expansion, J. Travel Med. 25 (suppl_1) (2018) S16–S26, https://doi.org/10.1093/jtm/tay009.
[9] E. Konishi, T. Suzuki, Ratios of subclinical to clinical Japanese encephalitis (JE) virus infections in vaccinated populations: evaluation of an inactivated JE vaccine by comparing the ratios with those in unvaccinated populations, Vaccine 21 (1–2) (2002) 98–107, https://doi.org/10.1016/s0264-410x(02)00433-4.
[10] T. Nguyen-Tien, A. Lundkvist, J. Lindahl, Urban transmission of mosquito-borne flaviviruses - a review of the risk for humans in Vietnam, Infect. Ecol. Epidemiol. 9 (1) (2019) 1660129, https://doi.org/10.1080/20008686.2019.1660129.
[11] J.F. Lindahl, K. Stahl, J. Chirico, S. Boqvist, H.T. Thu, U. Magnusson, Circulation of Japanese encephalitis virus in pigs and mosquito vectors within Can Tho city, Vietnam, Plos Neglect, Trop. Dis. 7 (4) (2013) e2153, https://doi.org/10.1371/journal.pntd.0002153.
[12] C. Cui, Y. Zhang, J. Song, Analysis of the epidemic situation of statutory infectious diseases in Xicheng District, Journal of Preventive Medicine 30 (1) (2018) 89–90.
[13] J. Nealon, A.F. Taurel, S. Yoksan, et al., Serological evidence of Japanese encephalitis virus circulation in asian children from dengue-endemic countries, J. Infect. Dis. 219 (3) (2019) 375–381, https://doi.org/10.1093/infdis/jiy513.
[14] J.M. Medlock, A.G. Vaux, Impacts of the creation, expansion and management of English wetlands on mosquito presence and abundance - developing strategies for future disease mitigation, Parasites Vectors 8 (2015) 142, https://doi.org/10.1186/s13071-015-0751-3.
[15] J. Lindahl, J. Chirico, S. Boqvist, H.T. Thu, U. Magnusson, Occurrence of Japanese encephalitis virus mosquito vectors in relation to urban pig holdings, Am. J. Trop. Med. Hyg. 87 (6) (2012) 1076–1082, https://doi.org/10.4269/ajtmh.2012.12-0315.
[16] H. Shimoda, Y. Ohno, M. Mochizuki, H. Iwata, M. Okuda, K. Maeda, Dogs as sentinels for human infection with Japanese encephalitis virus, Emerg. Infect. Dis. 16 (7) (2010) 1137–1139, https://doi.org/10.3201/eid1607.091757.
[17] T. Nguyen-Tien, A.N. Bui, J. Ling, et al., The distribution and composition of vector abundance in hanoi city, Vietnam: association with livestock keeping and flavivirus detection, Viruses 13 (11) (2021), https://doi.org/10.3390/v13112291.
[18] G. Le Flohic, V. Porphyre, P. Barbazan, J.P. Gonzalez, Review of climate, landscape, and viral genetics as drivers of the Japanese encephalitis virus ecology, Plos Neglect. Trop. Dis. 7 (9) (2013) e2208, https://doi.org/10.1371/journal.pntd.0002208.
[19] N. Gupta, K. Chatterjee, S. Karmakar, S.K. Jain, S. Venkatesh, S. Lal, Bellary, India achieves negligible case fatality due to Japanese encephalitis despite no vaccination: an outbreak investigation in 2004, Indian J. Pediatr. 75 (1) (2008) 31–37.
[20] S. Song, H. Yao, Z. Yang, Z. He, Z. Shao, K. Liu, Epidemic changes and spatio-temporal analysis of Japanese encephalitis in shaanxi province, China, 2005-2018, Front. Public Health 8 (2020) 380, https://doi.org/10.3389/fpubh.2020.00380.
[21] S. Zhang, W. Hu, X. Qi, G. Zhuang, How socio-environmental factors are associated with Japanese encephalitis in shaanxi, China-a bayesian spatial analysis, Int. J. Environ. Res. Public Health 15 (4) (2018), https://doi.org/10.3390/ijerph15040608.
[22] S. Zhao, Y. Li, S. Fu, et al., Environmental factors and spatiotemporal distribution of Japanese encephalitis after vaccination campaign in Guizhou Province, China (2004-2016), BMC Infect. Dis. 21 (1) (2021) 1172, https://doi.org/10.1186/s12879-021-06857-3.
[23] H.Y. Tian, P. Bi, B. Cazelles, et al., How environmental conditions impact mosquito ecology and Japanese encephalitis: an eco-epidemiological approach, Environ. Int. 79 (2015) 17–24, https://doi.org/10.1016/j.envint.2015.03.002.
[24] K.P. Suresh, A. Nayak, H. Dhanze, et al., Prevalence of Japanese encephalitis (JE) virus in mosquitoes and animals of the Asian continent: a systematic review and meta-analysis, J. Infect. Public Health 15 (9) (2022) 942–949, https://doi.org/10.1016/j.jiph.2022.07.010.

[25] N.H. Kim, W.G. Lee, E.H. Shin, J.Y. Roh, H.C. Rhee, M.Y. Park, Prediction forecast for Culex tritaeniorhynchus populations in Korea, Osong Public Health Res Perspect 5 (3) (2014) 131–137, https://doi.org/10.1016/j.phrp.2014.04.004.
[26] J.B. Gingrich, A. Nisalak, J.R. Latendresse, et al., Japanese encephalitis virus in Bangkok: factors influencing vector infections in three suburban communities, J. Med. Entomol. 29 (3) (1992) 436–444.
[27] J. Metelka, C. Robertson, C. Stephen, Japanese encephalitis: estimating future trends in Asia, AIMS Public Health 2 (4) (2015) 601–615, https://doi.org/10.3934/publichealth.2015.4.601.
[28] T.V. Ha, W. Kim, T. Nguyen-Tien, et al., Spatial distribution of Culex mosquito abundance and associated risk factors in Hanoi, Vietnam, Plos Neglect, Trop. Dis. 15 (6) (2021) e0009497, https://doi.org/10.1371/journal.pntd.0009497.
[29] C. Li, G. Xiao-Xia, H. En-Jiong, D. Yan-De, Z. Tong-Yan, New breeding of Culex tritaeniorhynchus in city, Chin. J. Vector Biol. Control 18 (1) (2007) 31.
[30] B. Lu, H. Chen, F. Qu, Fauna Sinica: Insecta, vol. 8, Science Press, Beijing, China, 1997. Diptera, Culicidae.
[31] E. Nunez, E.W. Steyerberg, J. Nunez, [Regression modeling strategies], Rev. Esp. Cardiol. 64 (6) (2011) 501–507, https://doi.org/10.1016/j.recesp.2011.01.019.
[32] E. Vittinghoff, C.E. Mcculloch, Relaxing the rule of ten events per variable in logistic and Cox regression, Am. J. Epidemiol. 165 (6) (2007) 710–718, https://doi.org/10.1093/aje/kwk052.
[33] T. Zhao, R. Xue, Integrated mosquito management in rice field in China, Wetl. Ecol. Manag. 30 (5) (2022) 963–973, https://doi.org/10.1007/s11273-021-09840-6.
[34] Z. Ming-Hao, C. Hong-Liang, Z. Ai-Jun, et al., Research on the species composition of urban mosquitoes before and after integrated management, Acta Parasitology et Medica Entomologica Sinica 18 (4) (2011) 220–224, https://doi.org/10.3969/j.issn.1005-0507.2011.04.005.
[35] L. Mei-De, T. Ying, Z. Yong, L. Ting, Z. Xiao-Peng, Time and space dynamics of mosquitoes in Beijing from 2013 to 2017, Capital Journal of Public Health 13 (2) (2019) 62–65.
[36] B.L. Lu, FAUNA SINICA. INSECTA. Vol.8. Diptera: Culicidae I, Science Press, Beijing, 1997.
[37] S.J. Zhang, T.Z. Ma, Z.Q. Li, et al., Surveillance on Culex tritaeniorhynchus from 2011 to 2013 in surrounding areas of Beijing capital international airport, China, Chin. J. Vector Biol. Control 25 (4) (2014) 323–325, https://doi.org/10.11853/j.issn.1003.4692.2014.04.010, 329.
[38] Z. Hong-Jiang, G. Jun-Qi, T. Cheng-Jun, Z. Zheng, L. Mei-De, Z. Yong, Distribution and seasonality of Culex tritaeniorhynchus in Chaoyang district, Beijing, Chin. J. Vector Biol. Control 27 (2) (2016) 148–150, https://doi.org/10.11853/j.issn.1003.8280.2016.02.014.
[39] L. Mei-De, Z. Yong, T. Ying, et al., Monitoring and analysis of the mosquito vector of Japanese B encephalitis in BEIJING olympic forest park, Acta Parasitology et Medica Entomologica Sinica 28 (3) (2021) 153–158, https://doi.org/10.3969/j.issn.1005-0507.2021.03.004.
[40] F. Zhu, Z. Jiang, Clinical report of 414 cases of Japanese encephalitis in children seen in Beijing, Chinese Journal of Pediatrics 4 (3) (1953).
[41] W.Y. Ji, M.P. Sun, Y. Ceng, H.R. Zhang, Epidemiological characteristics of Japanese encephalitis B in Beijing,2000-2007, CHINA PREVENTIVE MEDICINE 9 (12) (2008) 1070–1072, https://doi.org/10.3969/j.issn.1009-6639.2008.12.016.
[42] P. Masuoka, T.A. Klein, H.C. Kim, et al., Modeling the distribution of Culex tritaeniorhynchus to predict Japanese encephalitis distribution in the Republic of Korea, Geospat. Health 5 (1) (2010) 45–57.
[43] Y. Zhou, X.P. Min, P. Liang, Analysis of meteorological causes of epidemic Japanese encephalitis in Qiandongnan Prefecture in July 1971, Journal of Guizhou Meteorology 35 (3) (2011) 24–27.
[44] L. Xiao-Bo, W.U. Hai-Xia, Y. Wen-Wu, et al., Surveillance for Culex tritaeniorhynchus in China, 2006-2012, Disease Surveillance 29 (4) (2014) 281–286, https://doi.org/10.3784/j.issn.1003-9961.2014.04.008.
[45] E. Wermelinger, C. Benigno, R. Machado, et al., Mosquito population dynamic (Diptera: Culicidae) in a eutrophised dam, Braz. J. Biol. 72 (4) (2012) 795–799.
[46] B. Liu, X. Gao, J. Ma, Z. Jiao, J. Xiao, H. Wang, Influence of host and environmental factors on the distribution of the Japanese encephalitis vector Culex tritaeniorhynchus in China, Int. J. Environ. Res. Public Health 15 (9) (2018), https://doi.org/10.3390/ijerph15091848.
[47] S.S. Caglar, B. Alten, R. Bellini, F.M. Simsek, S. Kaynas, Comparison of nocturnal activities of mosquitoes (Diptera: Culicidae) sampled by New Jersey light traps and CO2 traps in Belek, Turkey, J. Vector Ecol. 28 (1) (2003) 12–22.
[48] D. Sanders, R. Kehoe, K. Tiley, et al., Artificial nighttime light changes aphid-parasitoid population dynamics, Sci. Rep. 5 (2015) 15232, https://doi.org/10.1038/srep15232.
[49] S. Rund, L.F. Labb, O.M. Benefiel, G.E. Duffield, Artificial light at night increases Aedes aegypti mosquito biting behavior with implications for arboviral disease transmission, Am. J. Trop. Med. Hyg. 103 (6) (2020) 2450–2452, https://doi.org/10.4269/ajtmh.20-0885.
[50] C.M. Barker, B.G. Bolling, C.G. Moore, L. Eisen, Relationship between distance from major larval habitats and abundance of adult mosquitoes in semiarid plains landscapes in Colorado, J. Med. Entomol. 46 (6) (2009) 1290–1298.
[51] G. Guzzetta, F. Vairo, A. Mammone, et al., Spatial modes for transmission of chikungunya virus during a large chikungunya outbreak in Italy: a modeling analysis, BMC Med. 18 (1) (2020) 226, https://doi.org/10.1186/s12916-020-01674-y.
[52] L.P.J. Martinez-De, R. Soriguer, J.C. Senar, J. Figuerola, R. Bueno-Mari, T. Montalvo, Mosquitoes in an urban zoo: identification of blood meals, flight distances of engorged females, and avian malaria infections, Front. Vet. Sci. 7 (2020) 460, https://doi.org/10.3389/fvets.2020.00460.
[53] L.K. Estep, N.D. Burkett-Cadena, G.E. Hill, R.S. Unnasch, T.R. Unnasch, Estimation of dispersal distances of Culex erraticus in a focus of eastern equine encephalitis virus in the southeastern United States, J. Med. Entomol. 47 (6) (2010) 977–986.